2007). Such cell behaviors imply that the cells are alive and not dead. Unless escaping from a host cell, an internalized cell is eventually degraded through the autophagy-protein-dependent fusion of lysosomes to the vacuolar membranes surrounding the internalized cell (Florey *et al.* 2011). It has been reported that when a host cell enters mitosis with an internalized cell, the internalized cell can prevent the cytokinesis of the host cell, resulting in the generation of a binucleate cell, potentially contributing to aneuploidy (Krajcovic *et al.* 2011). Therefore, cell-in-cell structures may be one of the phenotypes representing some kind of genomic instability.

Although internalized cells inside host cells have been analyzed from the point of view of cell death, little is known about how and which cells, the engulfing host cells or the invading inhabitant cells, take the first initiative in the formation of the cell-in-cell structures. In this article, we report the establishment of a mutagenized cell line promoting the formation of cell-in-cell structures in the suspension culture condition. In this cell line, change in the culture condition reduced the frequency of formation of the cell-in-cell structures. Furthermore, the events of both engulfment and invasion involved in the formation of the cell-in-cell structures were promoted. This observation shows that the mutagenized cell line has the ability to exhibit both enhanced engulfment and enhanced invasion and suggests that the cellular environment has a key role in determining which of the two events, engulfment or invasion, predominates.

Results

Induction of cell-in-cell structures in the HCT116 cell line

Entosis is induced in the suspension culture condition and has been observed in various cell lines (Overholtzer *et al.* 2007). We had noticed, during the counting of a large number of the cells (Kahyo *et al.* 2011), that HCT116, a human colorectal cancer cell line, showed an extraordinarily small number of cell-in-cell structures on adhesive-coated culture dishes. Therefore, first of all, we examined the ability of HCT116 to form cell-in-cell structures under the suspension culture condition using a nonadhesive coating of the culture dishes (Fig. 1A). To avoid confusion, the word 'cell-in-cell' structures in this article is principally used for the nested doll-like structures, even if other words, such as entosis, may have been suitable. We counted the formation of both partial and complete forms, the former representing either the internalization or the extrusion process. The observations showed that the formation of both the partial and complete forms of the cell-in-cell structures was promoted in the suspension culture condition on a non-adhesive-coated surface. The number of cell-in-cell structures was increased by fivefold in suspension culture on a non-adhesive-coated culture dish (Student's *t*-test, $P = 0.005$). This result was consistent with a previous report on entosis (Overholtzer *et al.* 2007), which indicated that entosis of MCF10A and MCF7 cells occurred at a high frequency in suspension culture. However, in the HCT116 cell line, the cell-in-cell structures occurred at a frequency of approximately 1%, and the number of cell-in-cell structures was actually much smaller than that in the MCF7 cells (Fig. 1B; Student's *t*-test, $P < 0.001$).

Mutagenized cell line showing enhanced formation of cell-in-cell structures

The above observation suggests that an unknown mechanism suppresses the formation of cell-in-cell structures even under the suspension culture condition in the HCT116 cell line. Then, we attempted to boost the ability of the HCT116 cells to form cell-in-cell structures using the chemical mutagenesis method (Fig. 2A). HCT116 cells were treated for 8 h with ICR-191, an acridine derivative, which predominantly induced frameshift mutations (Cariello *et al.* 1990). ICR-191 was used at a concentration of 6.2 μg/mL, which killed half of the cells (Fig. S1 in Supporting Information). After colony formation, the colonies were picked up and cultured, and the cultured cells were distributed into two plates for subculture and cell-in-cell assay. In the assay for the cell-in-cell structures, the mutagenized cells were screened by microscopic observation. Four clones showing a relatively high frequency of cell-in-cell structures were selected of 144 clones on the assay plate, and cell counting showed that the 9F clone showed the largest number of cell-in-cell structures among the four clones (Fig. 2B). The 9F clone was amplified from the subculture plate and used for the second round of screening with ICR-191. Five clones with a relatively high frequency of cell-in-cell structures were selected of 144 single cell colonies from 9F clone. Finally, the cell clone, 9F-11A, which showed the highest ability to form cell-in-cell structures in the suspension culture condition, was

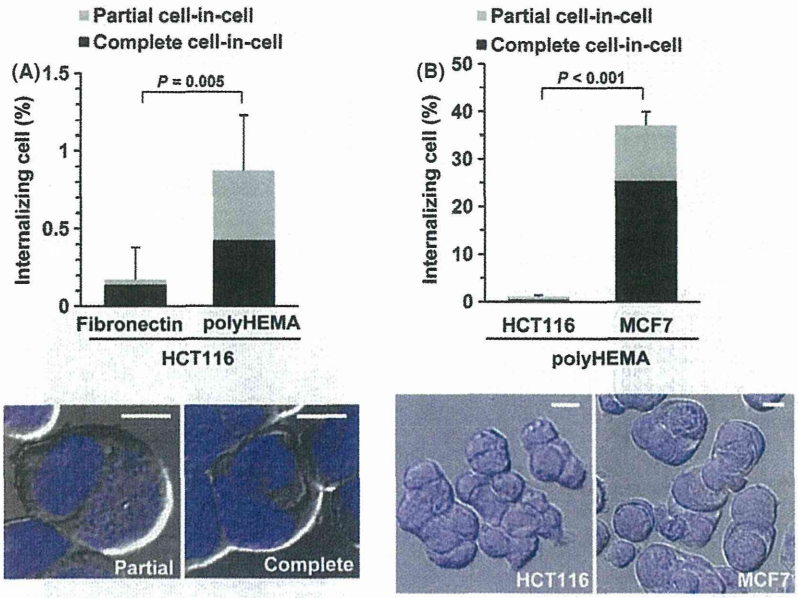

Figure 1 Cell-in-cell formation in the HCT116 cells. (A) HCT116 human colorectal cancer cells (12.5 cells/100 μm^2) were plated on to a fibronectin-coated (adhesive) or polyHEMA-coated (nonadhesive) dish and cultured for 14 h. The cells on the polyHEMA-coated dish were transferred on a silane-coated glass slip and centrifuged for attachment to the slip. The cells were fixed with paraformaldehyde and stained with DAPI. Cell-in-cell structures were observed and counted using differential interference contrast (DIC) optics and confocal laser scanning. (B) HCT116 cells (12.5 cells/100 μm^2) and MCF7 human breast cancer cells (8 cells/100 μm^2) were plated on to polyHEMA-coated dish and cultured for 14 h. The panels on the bottom are the images of representative cell-in-cell structures. Bar = 10 μm. The numbers of cells count in five (A) or six (B) experiments were as follows (cell-in-cell/total): 5/2697 (fibronectin) and 16/1792 (polyHEMA) in (A); and 35/3099 (HCT116) and 1118/3022 (MCF7) in (B). Data represent the mean ± SD of the total rate of complete and partial cell-in-cell structures.

acquired (Figs. 2B and 2C). 9F-11A showed a more than 10-fold higher number of cell-in-cell structures as compared to the parent HCT116 cells, and it was actually observed that the host cells contained whole cell bodies (Fig. 2D, left panel). Furthermore, time-lapse imaging analysis indicated that the internalized cells probably remained alive in the host cells for at least several hours (Fig. 2E, and Movie S1 in Supporting Information). Thus, the cell clone, 9F-11A, showing enhanced formation of the cell-in-cell structures, was generated from the HCT116 cell lines by the chemical mutagenesis method.

Culture conditions affecting the formation of the cell-in-cell structures in 9F-11A

On the cell-attachment dishes, the 9F-11A cells often showed different cell shapes as compared to the parent cells (Fig. 3A). Some 9F-11A cells extended slender pseudopodia, the lengths of which were sometimes twice to three times the sizes of the cell bodies themselves, whereas the parent cells rarely showed these features. As the altered regulation of actin polymerization was expected in the 9F-11A cells, the cell-in-cell assay using cytochalasin B (CytB), which is an inhibitor of actin polymerization and has been shown to be involved in the process of formation of the cell-in-cell structures (Lugini *et al.* 2006; Takeuchi *et al.* 2010), was carried out. The rate of the cell-in-cell structures was significantly lower in the CytB-treated cells than in the cells without the treatment of CytB (Fig. 3B; Student's *t*-test, $P = 0.002$ in the samples of 0.2 and 0.8 μg/mL of CytB). This result shows that the actin polymerization pathway is involved in the process of formation of the cell-in-cell structures in the 9F-11A cells. In contrast, similar to the case for the parent cell line, formation of the cell-in-cell structures in 9F-11A seemed to be suppressed on adhesive-coated dishes. Then, we examined the culture condition that would prevent the formation of cell-in-cell structures in 9F-11A, because the presence of cell-in-cell structures at a high frequency can cause genomic instability of the host cells, and we needed to subculture the 9F-11A

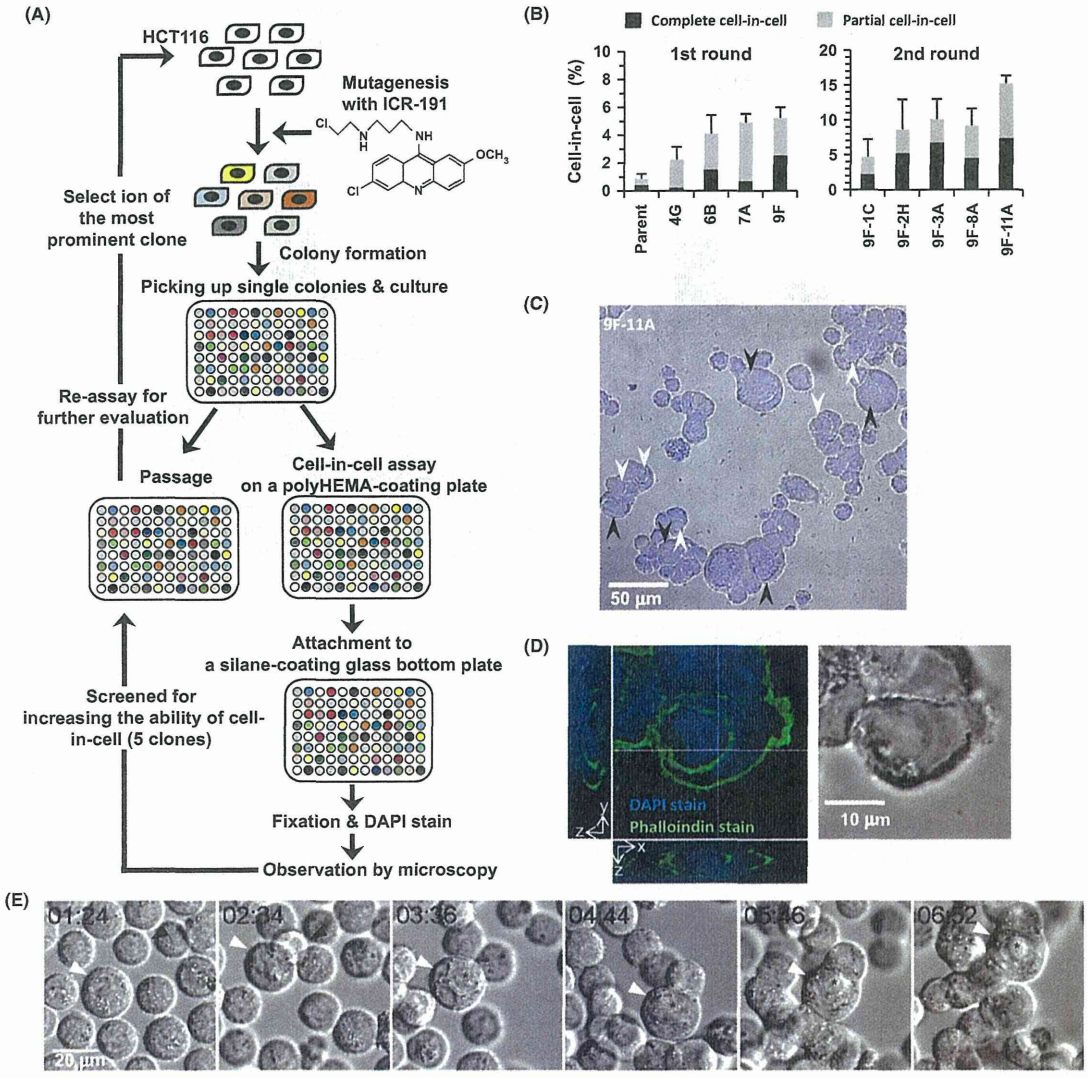

Figure 2 Establishment of a cell line showing enhanced formation of the cell-in-cell structures. (A) Screening of clones showing enhanced formation of cell-in-cell structures. HCT116 cells were exposed to 6.2 μg/mL of ICR-191, known as a frameshift mutagen, for 8 h. The culture medium was replaced with fresh medium, and the cells were recultured for 24 h. The cells were trypsinized and plated on ϕ100-mm dishes at a low density. After the colony formation, 144 single colonies were picked up, amplified and passaged on master and assay plates. The cells on the assay plate were transferred to a silane-coated glass-bottomed plate after culture for 14 h, centrifuged, fixed and stained with DAPI. Several clones were selected and furthermore evaluated. These mutagenesis/screening steps were repeated again. (B) The graph shows the results of the first and second round of screening. The clone 9F was used for the second round of screening. At least 1000 cells were counted. (C) Cell-in-cell structures of 9F-11A cells formed in the screening assay. DIC and DAPI fluorescence (blue) images of 9F-11A are merged. Black and white arrowheads indicate complete and partial cell-in-cell structures, respectively. (D) A whole image of a representative cell-in-cell structure. After fixation, cells were stained with DAPI (blue) and phalloidin–Alexa 488 (green). The right panel shows a light field. (E) Time-lapse imaging of internalization in the 9F-11A cells. DIC images were captured during cell culture on polyHEMA-coated glass-bottomed dishes at 2-min intervals. Black and white arrows show future internalized and host cells, respectively. The asterisk shows a completely internalized cell. Time zero corresponds to the initiation of the image capture immediately after plating of the cells on to a polyHEMA-coated glass-bottomed dish. The numbers of cells count in five experiments were as follows (cell-in-cell/total): 30/3372 (parent), 69/3329 (4G), 130/3344 (6B), 158/3257 (7A), 142/2757 (9F), 52/980 (9F-1C), 88/1084 (9F-2H), 60/678 (9F-3A), 105/1159 (9F-8A) and 186/1223 (9F-11A). Data represent the mean ± SD of the total rate of complete and partial cell-in-cell structures.

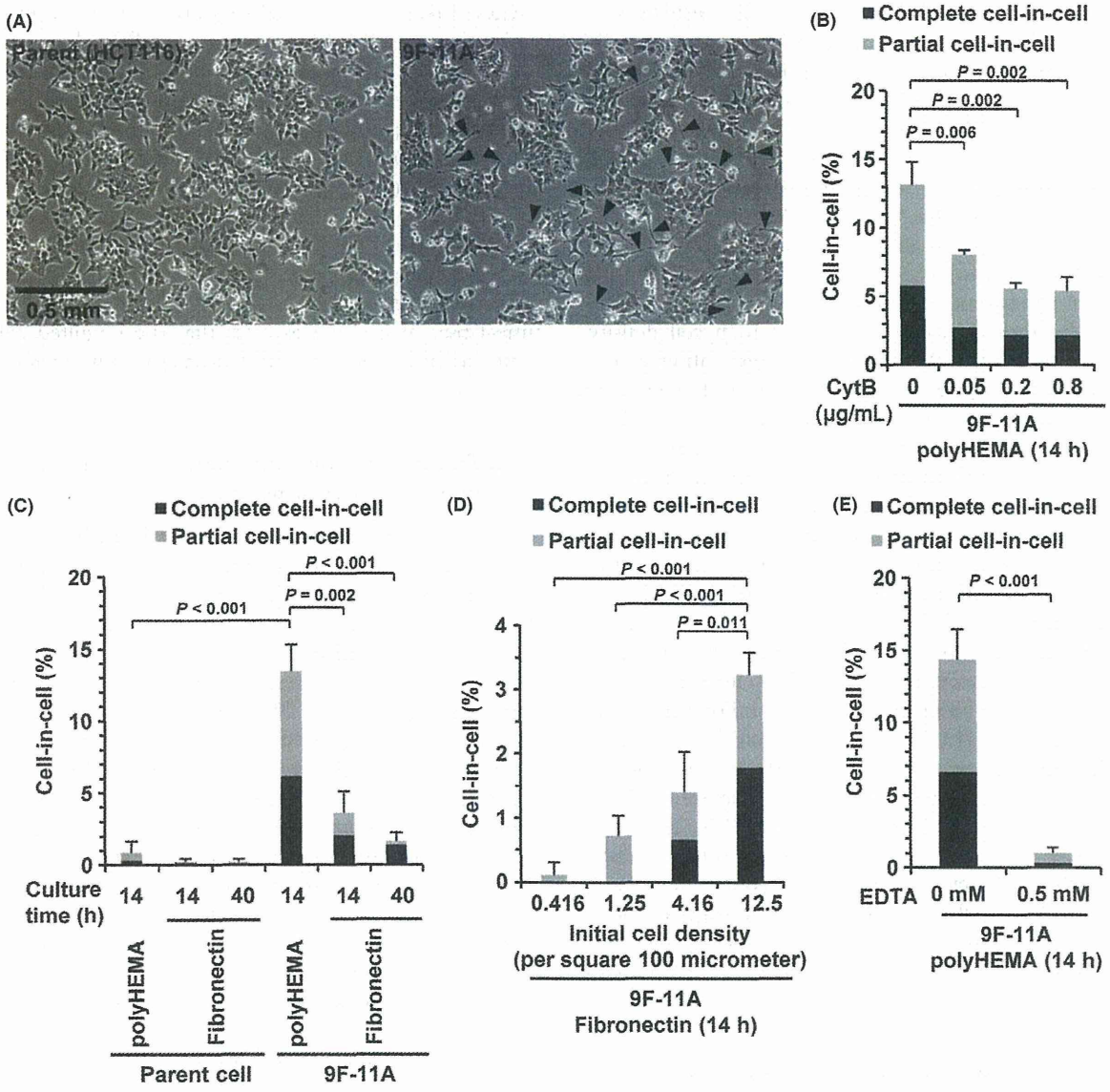

Figure 3 Culture conditions affecting the frequency of formation of cell-in-cell structures in 9F-11A. (A) Morphological differentiation between parent and 9F-11A cells. Parent (left) and 9F11-A (right) cells were subcultured under the cell-attachment condition. Arrows indicate representative slender pseudopodia. (B) Formation of cell-in-cell structures in the presence of cytochalasin B (CytB), an inhibitor of actin polymerization. 9F-11A cells were plated on polyHEMA-coated dishes in medium containing 0.05, 0.2 and 0.8 μg/mL of CytB. (C) Formation of cell-in-cell structures in the 9F-11A cells cultured on an adhesive-coated surface. Parent and 9F-11A cells were plated on fibronectin-coated and polyHEMA-coated dishes. (D) Formation of cell-in-cell structures in a cell density-dependent manner. 9F-11A cells were plated on fibronectin-coated dishes at the indicated cell densities and cultured for 14 h. (E) Suppression of the formation of cell-in-cell structures by EDTA chelation. 9F-11A cells were plated onto polyHEMA-coated dishes in medium containing 0.5 mM EDTA and cultured for 14 h. The numbers of cells count in three experiments were as follows (cell-in-cell/total): 152/1154 (CytB 0 μg/mL), 86/1074 (CytB 0.05 μg/mL), 67/1196 (CytB 0.2 μg/mL) and 58/1070 (CytB 0.8 μg/mL) in (B); 5/630 (parent polyHEMA), 3/1083 (parent fibronectin for 14 h), 3/1403 (parent fibronectin for 40 h), 89/690 (9F-11A-polyHEMA), 24/765 (9F-11A-fibronectin for 14 h) and 14/867 (9F-11A-fibronectin for 40 h) in (C); 1/566 (cell density 0.416), 4/566 (1.25), 8/539 (4.16) and 24/743 (12.5) in (D); and 90/625 (EDTA 0 mM) and 6/559 (0.5 mM) in (E). Data represent the mean ± SD of the total rate of complete and partial cell-in-cell structures.

cells under a little stimulation for the formation of cell-in-cell structures as possible. As expected, on the adhesive-coated dishes, the number of cell-in-cell structures in the 9F-11A cells decreased to less than one-fourth of that in the suspension culture condition (Fig. 3C; Student's *t*-test, $P < 0.001$ in the 9F-11A cells cultured on the adhesive-coated dishes for 40 h). Nonetheless, in the 9F-11A cells, the cell-in-cell structures occurred at a frequency of more than 1% on the adhesive-coated surface, being still higher than that for the parent cell line under the same condition. This was thought to be due to the high cell density (12.5 cells/100 μm^2) immediately after plating of the cells on the culture dishes, when the cells were still not attached to the bottom. The cell density of 12.5 cells/100 μm^2 corresponds to the cell crowdedness indicated in the first panel of Figure 2D, and frequent cell–cell contacts seemed to affect the formation of the cell-in-cell structures. In fact, the lower the culture cell density of the 9F-11A cells, the lower the number of cell-in-cell structures observed (Fig. 3D; Student's *t*-test, $P < 0.001$ in the cell density of 0.416 cells/100 μm^2). Furthermore, formation of the cell-in-cell structures in the 9F-11A cells was strongly suppressed in suspension culture condition even at the cell density of 12.5 cells/100 μm^2, by treatment with the chelating agent EDTA (ethylenediaminetetraacetic acid), which inhibits the formation of cell-in-cell structures (Overholtzer *et al.* 2007) (Fig. 3E; Student's *t*-test, $P < 0.001$). These results indicate that cell–cell contacts are indispensable for the formation of cell-in-cell structures and that plating at a low density on an adhesive-coated dish prevents the formation of the cell-in-cell structures to a great extent and is suitable for subculture of the 9F-11A cells.

Live cell behaviors of the internalized cells

In the cell-in-cell structures, the cells have been reported to remain alive after they are internalized (Lugini *et al.* 2006; Fais 2007; Overholtzer *et al.* 2007). Therefore, we focused on the behaviors of the internalized 9F-11A cells. Figure 4A and Movie S2 in Supporting Information show the time-lapse images of the internalization process of multiple cells (black arrowheads 1–3). Cell '1', which had been internalized by the host cell (white arrowhead), moved behind another internalized cell '2' and extruded out of the host cell simultaneously with the internalization of cell '3'. Furthermore, cell '1' divided into two daughter cells '1a' and '1b' immediately after emerging from the host cells. These scenes suggest that cell '1' was alive during both the entry and exit processes. In other cases, cells sinking into another cell sometimes showed pseudopodial dynamics in the process of formation of the cell-in-cell structures (Fig. 4B and Movies S3 and S4 in Supporting Information). The active pseudopodia were observed at the opposite side of the host cell, and the sinking cell seemed to be escaping from the host cell, or otherwise, thrashing toward the host cell. Although offense and defense between the outside and inside cells could not be elucidated from the time-lapse images, it was clear that the engulfed cells were still alive and active at least at the time of internalization.

Engulfment and invasion events in the cell-in-cell phenomenon observed in 9F-11A

The above results establish beyond doubt that the formation of cell-in-cell structures is promoted in the 9F-11A cells, but it still remained unclear which of the two processes, engulfment or invasion, was promoted because of the homotypic cell-in-cell event. Therefore, a labeling assay with fluorescent probes was carried out. HCT116 and 9F-11A cells were labeled with red and green fluorescent probes, respectively, and the cells were mixed, cultured in suspension condition and observed under a fluorescence microscope. As compared to the number of parent/parent (outside/inside) pairs, the number of the parent/9F-11A pairs was increased by approximately twofold (Fig. 5; Student's *t*-test, $P = 0.008$), as also that of the 9F-11A/9F-11A pairs (Student's *t*-test, $P = 0.006$). These results show that invasion events are increased by twofold in the 9F-11A cells as compared with that in the parent cells. Similarly, engulfment events were estimated to be increased by approximately fivefold in the 9F-11A cells as compared with that in the parent cells (Fig. 5; Student's *t*-test, $P < 0.001$ between parent/parent and 9F-11A/parent and between parent/9F-11A and 9F-11A/9F-11A). These results indicate that the events of both engulfment and invasion are activated in the 9F-11A cells and that 9F-11A cells show enhanced ability for both engulfment and invasion.

Discussion

Mutagenesis using ICR-191 has often been preferred to obtain cell clones of various phenotypes, such as resistance to virus infection (Bruce *et al.* 2005), aberrant cell replication (Zientek-Targosz *et al.* 2008) and

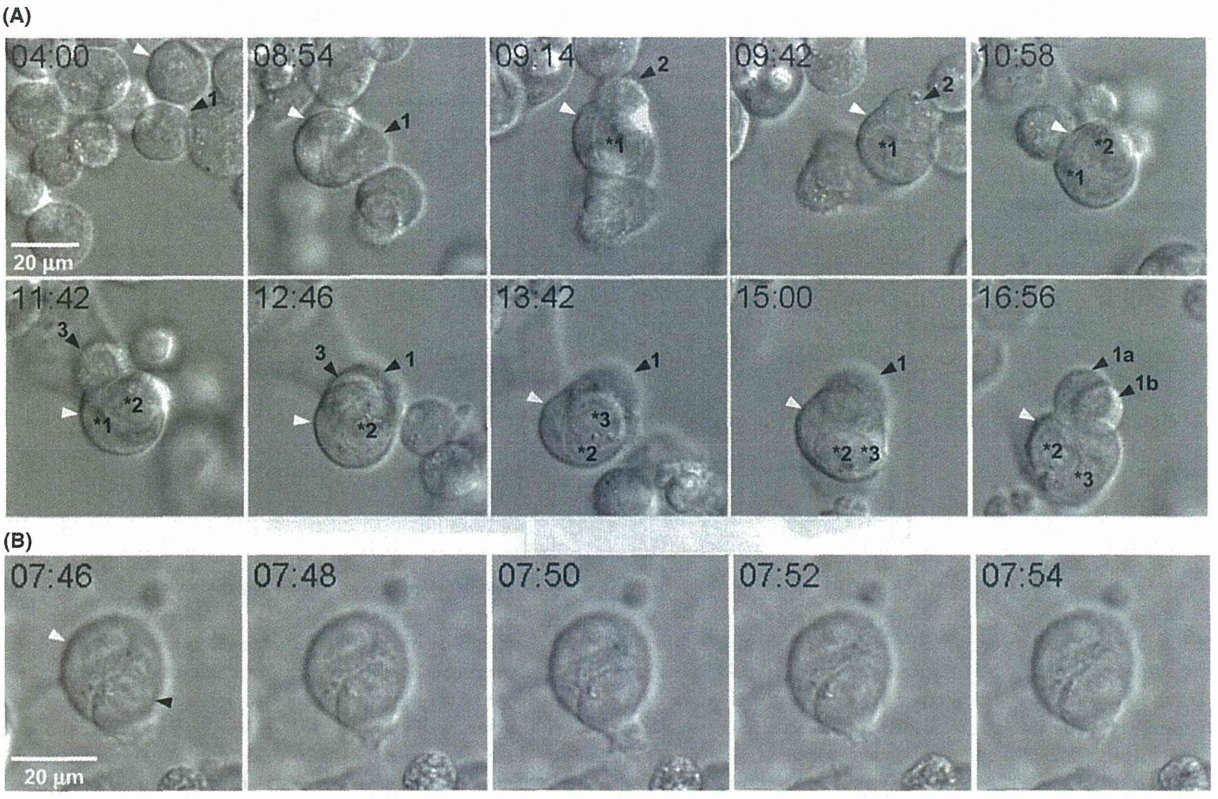

Figure 4 Live cell behaviors of the internalized cells. (A) Multiple cells (numbers 1–3) were internalized in the same host cell. Black and white arrows show future internalized and host cells, respectively. Arrow '1' cell divided into '1a' and '1b' cells immediately after emerging from the host cell. The asterisk shows a completely internalized cell. (B) Pseudopodial dynamics of a cell sinking into another cell. Time zero corresponds to the initiation of the image capture immediately after plating of the cells on a polyHEMA-coated glass-bottomed dish.

defective molecular signaling (Kohno *et al.* 2008). In this article, microscopic observation was used to screen cell clones showing enhanced formation of cell-in-cell structures. Cell-in-cell structures show remarkably varied appearances because of the dynamic cell behaviors, including partial and multiple internalizations. Therefore, there was no better method than using microscopic observational selection as a screening method to assay the cell-in-cell phenomenon. Another advantage of this method was that no second validation of the cell-in-cell structures was necessary due to the direct observation.

Although the mutagenized sites in the 9F-11A cells are soon expected to be identified through genomic analysis with a high-throughput DNA sequence, some putative molecules affected by mutagenesis can be presumed ahead of the genomic analysis. Active pseudopodia were observed during the process of formation of the cell-in-cell structures in the 9F-11A cells (Fig. 4B and Movies S3 and S4 in Supporting Information), and slender pseudopodia, which are rarely observed in the parent HCT116 cell line, were also often found under the cell-attachment culture condition (Fig. 3A). These findings suggest that the activities of actin regulatory proteins are aberrantly altered in the 9F-11A cells. Interestingly, several groups have reported that aberration of the actin polymerization pathway affects the frequency of formation of cell-in-cell structures: treatment with cytochalasin, an inhibitor of actin polymerization, suppressed active invasion of gastric carcinoma cells by the cytotoxic regulatory T-cell line HOZOT (Takeuchi *et al.* 2010); down-regulation of Rho-ROCK signaling led to a decrease in the cell invasion of MCF10A in suspension culture condition (Overholtzer *et al.* 2007); and expression of a deletion mutant form of ezrin, an actin-binding protein, reduced the cannibalistic activity of metastatic mela-

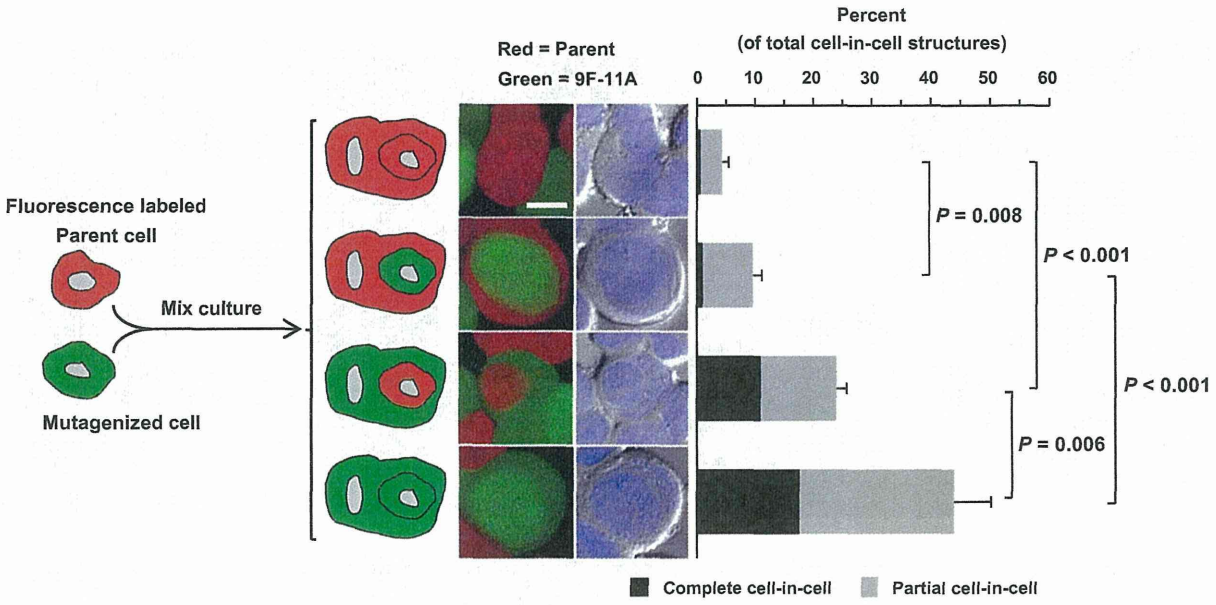

Figure 5 Increased ability of the 9F-11A cells for both engulfment and invasion involved in the formation of the cell-in-cell structures. Parent and 9F-11A cells were labeled with red and green fluorescent probes, respectively. The labeled cells were mixed, cultured in suspension condition and observed under a fluorescence microscope. The percent of cell-in-cell structures of each pair pattern per total number of cell-in-cell structures was represented. Fluorescence (left) and DIC (right) images are shown. Bar = 10 μm. The numbers of cell-in-cell structures in the three experiments were as follows: 13 (outside/inside = parent/parent), 30 (parent/9F-11A), 74 (9F-11A/parent) and 140 (9F-11A/9F-11A). Data represent the mean ± SD of the total rate of complete and partial cell-in-cell structures.

noma cells directed at live lymphocytes (Lugini *et al.* 2006). The treatment of cytochalasin actually suppressed the formation of the cell-in-cell structures in the mutagenized cells (Fig. 3B). The treatment of cells with ICR-191 is, if anything, thought to cause loss-of-function mutation because of the frameshift-biased mutation spectrum (Cariello *et al.* 1990). Therefore, it can be speculated that the actin-related molecules suppressing the formation of the protuberant structures such as pseudopodia observed in Fig. 3A and Fig. 4B were targeted by the mutagenesis, resulting in the enhanced formation of the cell-in-cell structures, although it cannot be ruled out that increased pseudopodia formation in the 9F-11A cells is not involved in the formation of the cell-in-cell structures.

Although the number of cell-in-cell structures was reduced in the cell-attachment condition, the suppressive mechanism is still not clear. Interestingly, complete cell-in-cell structures seemed to be more resistant to reduction in the cell-attachment condition than partial cell-in-cell structures (Figs. 1A and 3C). This could be due to the time lag between the formation of the cell-in-cell structures and attachment to the bottom. Once the cells are attached to the bottom, the cell-in-cell events are certain to be suppressed, and few partial features of cell-in-cell structures would be observed after the attachment. In contrast, if the cells were able to slowly advance from partial cell-in-cell structures formed during floating in the culture medium to complete cell-in-cell structures even after attachment to the bottom, it would be reasonable to expect a large number of complete cell-in-cell features on the adhesive coating than partial cell-in-cell structures. On the contrary, under the condition of low cell density, only partial cell-in-cell forms were observed on adhesive-coated dishes (Fig. 3C). This would be due to the delay in cell–cell contacts during floating. At a low cell density, engulfment and invasion are not likely to occur until just before the attachment to the bottom, because it takes a long time for cell–cell contacts to be established in a cell-sparse space. Thus, since there would be little time for the formation of cell-in-cell structures after the attachment to the bottom, no complete cell-in-cell forms are observed at a low cell density.

In previous reports, cell-in-cell-engaged cells seemed to prefer either one of the events of engulfment or invasion (Lugini *et al.* 2006; Takeuchi *et al.* 2010), and the ability of the cells to exhibit both in the formation of the cell-in-cell structures has never been discussed. In this article, we established a cell line that showed enhanced ability for both engulfment and invasion. This fact raises the question of what determines the cell fate, engulfment or invasion, in each 9F-11A cell. One of the clues to answering this question could be related to the heterogeneity of the cultured cells. Even if a single cell is cultured, the population of proliferating cells will show heterogeneity of the cell characteristics, such as the cell body size and transcriptional profiling (Dey-Guha *et al.* 2011; Narsinh *et al.* 2011). Thus, in 9F-11A, differences in the cellular characteristics from a contact partner cell, or differences in the cellular environment, may determine the alternative cell fate of engulfment or invasion, synergistically with the intracellular pathway affected by the mutagenesis. This hypothesis about the influence of the cellular environment can also be applied to other cell lines, including ones that show strong preference to either engulfment or invasion. Even a cell showing a prominent invasive phenotype must be stimulated for engulfment in some cellular environments, although an innate property for invasion may dominate over the stimulus for engulfment in most cases. The power balance between an innate property and stimulus from a cellular environment would determine which of engulfment and invasion occurs in each cell and also characterize the features of the cell-in-cell phenomenon in each cell line. Furthermore, our finding that both engulfment and invasion were increased in the mutagenized cell line shows that cell-in-cell structures can be formed not only by either process of enhanced engulfment or invasion, but also by both of these processes. This will be a key concept for understanding the physiological and pathological roles of cell-in-cell formation *in vivo*. Engulfment and invasion have been reported as different concepts and to be individually associated with specific biological roles, such as nutrient supply to the host cell in an engulfment event, and cell death of the host cell in an invasion event (Lugini *et al.* 2006; Takeuchi *et al.* 2010). The idea that cell-in-cell structures can be formed through a mixed process of enhanced engulfment and enhanced invasion may imply that cell-in-cell structures are not always homogeneously associated with either one of the biological roles and that there is the possibility that cell-in-cell structures have heterogeneous features mediating various biological roles.

Details of the cell-in-cell phenomenon have yet to be investigated considering that cell-in-cell structures have been reported for a long time. In this article, the ability of the cells to show both enhanced invasion and engulfment involved in the formation of cell-in-cell structures was showed through characterization of the mutagenized cell line. An understanding of this ability will be helpful in appreciating its biological events involved in the occurrence of the cell-in-cell phenomenon. In addition, genomic analysis of the mutagenized cell line may be expected to show the molecular mechanisms underlying the occurrence of the cell-in-cell phenomenon in future.

Experimental procedures

Cell culture and cell-in-cell assay

The human colorectal cancer cell line HCT116 (CCL-247; purchase date, 11/16/2005; American Type Culture Collection, Manassas, VA, USA), having a relatively stable karyotype, and the breast cancer cell line MCF7 (HTB-22; purchase date, 4/2/2013; American Type Culture Collection) were cultured at 37°C in RPMI medium (Life Technologies, Carlsbad, CA, USA) containing 10% fetal bovine serum (Nichirei, Tokyo, Japan) and penicillin–streptomycin solution (Life Technologies), under 5% CO_2. For the cell-in-cell assay, cultured cells (12.5 cells/100 μm^2) were plated on fibronectin (adhesive; Becton Dickinson, Franklin Lakes, NJ, USA)-coated glass slips (Kahyo *et al.* 2011) or polyHEMA (2-hydroxyethyl methacrylate; non-adhesive; Sigma–Aldrich)-coated dishes (Overholtzer *et al.* 2007) and cultured for 14 h. Cytochalasin B (final 0.05, 0.2 or 0.8 μg/mL; Sigma–Aldrich) and EDTA (final 0.5 or 2 mM; Sigma–Aldrich) were added to the medium at the start of culture. The cells on polyHEMA-coated dishes were transferred on silane (Sigma–Aldrich, St Louis, MO, USA)-coated glass slips and centrifuged at 33 × *g* for 5 min. In the screening experiment, silane-coated glass-bottomed 96-well plates were used instead of silane-coated glass slips. The cells were fixed with 4% paraformaldehyde (Sigma–Aldrich) at room temperature for 15 min and stained with DAPI (Life Technologies).

Mutagenesis and screening experiments

To acquire cell clones mutagenized with ICR-191, HCT116 cells were treated with 6.2 μg/mL of ICR-191 (dissolved in sterile distilled water, Sigma–Aldrich) for 8 h, cultured in fresh medium for 1 day, trypsinized and recultured at a low cell density (5000–10 000 cells/ϕ100-mm dish). The medium was exchanged with fresh medium once every 3 days, and 144 single cell colonies were picked up after culture for 9 days. The picked clone cells were passaged on 96-well plates (Thermo Scientific, Bremen, Germany), and each clone was distributed

into two plates for subculture and the cell-in-cell assay. In the case of the cell-in-cell assay, the cells were cultured at a high density on polyHEMA-coated plates, and the mutagenized cells were screened for cell-in-cell structures by differential interference contrast (DIC) optics and confocal laser scanning (FV1000; Olympus, Tokyo, Japan); then, four clones showing a relatively high frequency of cell-in-cell structures were selected, and cell counting showed that the 9F clone showed the largest number of cell-in-cell structures among the four clones. The 9F clone was amplified from the subculture plate and used for the second round of screening with ICR-191. Five clones with a relatively high frequency of cell-in-cell structures were selected of 144 single cell colonies from 9F clone, and the 9F-11A clone was finally evaluated as the cell clone showing cell-in-cell structures at the highest frequency. 9F-11A cells were subcultured at a low initial cell density (1 cell/100 μm^2) and used for the subsequent assays.

Microscopic analysis

When multiple cells were internalized by the same host cell, all the internalized cells were counted. In Fig. 2D, the fixed cells were stained with Alexa 488–phalloidin (Life Technologies) and observed using the *z*-stack imaging system (BZ-9000; Keyence, Osaka, Japan). For time-lapse imaging, the cells were plated on to polyHEMA-coated glass-bottomed dishes and cultured with the incubator microscope (FCV100; Olympus) for 20 h. DIC optical images were captured at 2-min intervals. To cover the visual field of the cells moving up and down, five capture steps were set up in a 20-μm *z*-axis range. In Fig. 3A, the images on the cell-attachment dishes (TPP, Trasadingen, Switzerland) were captured by the inverted microscope (Eclipse TS100; Nikon, Tokyo, Japan). Image data were analyzed by the Image J software (version 1.43f; National Institutes of Health, Bethesda, MD, USA).

Mixed culture assay using fluorescence probes

Parent cells and mutagenized cells (9F-11A) were cultured in medium containing 1 μM of CellTracker dye CMTMR (red fluorescence; Life technologies) and CMFDA (green fluorescence; Life technologies) for 30 min, respectively. Then, the medium was exchanged for fresh medium, and the cells were recultured for 30 min. After trypsinization, both the parent and mutagenized cells were washed with fresh medium, mixed with each other in equal amounts (final 12.5 cells/100 μm^2), plated on to polyHEMA-coated dishes and cultured for 14 h. Fluorescence images were captured by the confocal laser scanning system (FV1000).

Statistical analysis

The Student's *t*-test was used at the significance level of 0.05 (Figs. 1 and 3E) to statistically analyze the average rate of cell-in-cell structures. The Bonferroni correction was carried out for multiple comparison adjustment, in which the significance levels were 0.016 (Figs. 3B–D) and 0.012 (Fig. 5). The statistical analysis was carried out using the R software environment (R Core Team 2013). The rate of cell-in-cell structures was defined as the number of cell-in-cell structures per total number of cells (Figs. 1, 2 and 3) or as the number of cell-in-cell structures of each pair pattern per total number of cell-in-cell structures (Fig. 5).

Acknowledgements

This work was supported by grants from the Takeda Science Foundation; Grants-in-Aid for the U.S.–Japan Cooperative Medical Science Program; the National Cancer Center Research and Development Fund; Grants-in-Aid for Young Scientists (B) from the Japan Society for the Promotion of Science [grant number 23790396]; Priority Areas from the Japanese Ministry of Education, Culture, Sports, Science and Technology [20014007, 22659072, 221S0001]; and Grants-in-Aid for Cancer Research from the Japanese Ministry of Health [23120201 and 10103838].

References

Bauchwitz, M.A. (1981) The bird's eye cell: cannibalism or abnormal division of tumor cells. *Acta Cytol.* **25**, 92.

Brouwer, M., de Ley, L., Feltkamp, C.A., Elema, J. & Jongsma, A.P. (1984) Serum-dependent "cannibalism" and autodestruction in cultures of human small cell carcinoma of the lung. *Cancer Res.* **44**, 2947–2951.

Bruce, J.W., Bradley, K.A., Ahlquist, P. & Young, J.A. (2005) Isolation of cell lines that show novel, murine leukemia virus-specific blocks to early steps of retroviral replication. *J. Virol.* **79**, 12969–12978.

Cariello, N.F., Keohavong, P., Kat, A.G. & Thilly, W.G. (1990) Molecular analysis of complex human cell populations: mutational spectra of MNNG and ICR-191. *Mutat. Res.* **231**, 165–176.

Dey-Guha, I., Wolfer, A., Yeh, A.C., G Albeck, J., Darp, R., Leon, E., Wulfkuhle, J., Petricoin, E.F. 3rd, Wittner, B.S. & Ramaswamy, S. (2011) Asymmetric cancer cell division regulated by AKT. *Proc. Natl Acad. Sci. USA* **108**, 12845–12850.

Fais, S. (2007) Cannibalism: a way to feed on metastatic tumors. *Cancer Lett.* **258**, 155–164.

Florey, O., Kim, S.E., Sandoval, C.P., Haynes, C.M. & Overholtzer, M. (2011) Autophagy machinery mediates macroendocytic processing and entotic cell death by targeting single membranes. *Nat. Cell Biol.* **13**, 1335–1343.

Humble, J.G., Jayne, W.H. & Pulvertaft, R.J. (1956) Biological interaction between lymphocytes and other cells. *Br. J. Haematol.* **2**, 283–294.

Iyer, V.K., Handa, K.K. & Sharma, M.C. (2009) Variable extent of emperipolesis in the evolution of Rosai Dorfman disease: Diagnostic and pathogenetic implications. *J. Cytol.* **26**, 111–116.

Kahyo, T., Iwaizumi, M., Shinmura, K., Matsuura, S., Nakamura, T., Watanabe, Y., Yamada, H. & Sugimura, H. (2011) A novel tumor-derived SGOL1 variant causes abnormal mitosis and unstable chromatid cohesion. *Oncogene* **30**, 4453–4463.

Kohno, T., Daa, T., Otani, H., Shimokawa, I., Yokoyama, S. & Matsuyama, T. (2008) Aberrant expression of BAFF receptor, a member of the tumor necrosis factor receptor family, in malignant cells of nonhematopoietic origins. *Genes Cells* **13**, 1061–1073.

Krajcovic, M., Johnson, N.B., Sun, Q., Normand, G., Hoover, N., Yao, E., Richardson, A.L., King, R.W., Cibas, E.S., Schnitt, S.J., Brugge, J.S. & Overholtzer, M. (2011) A non-genetic route to aneuploidy in human cancers. *Nat. Cell Biol.* **13**, 324–330.

Krysko, D.V. & Vandenabeele, P. (2010) Clearance of dead cells: mechanisms, immune responses and implication in the development of diseases. *Apoptosis* **15**, 995–997.

Lee, K.P. (1989) Emperipolesis of hematopoietic cells within megakaryocytes in bone marrow of the rat. *Vet. Pathol.* **26**, 473–478.

Lugini, L., Matarrese, P., Tinari, A., Lozupone, F., Federici, C., Iessi, E., Gentile, M., Luciani, F., Parmiani, G., Rivoltini, L., Malorni, W. & Fais, S. (2006) Cannibalism of live lymphocytes by human metastatic but not primary melanoma cells. *Cancer Res.* **66**, 3629–3638.

Martinez, M., Samms, M., Hendrix, T.M., Adeosun, O., Pezzano, M. & Guyden, J.C. (2007) Thymic nurse cell multicellular complexes in HY-TCR transgenic mice demonstrate their association with MHC restriction. *Exp. Biol. Med. (Maywood)* **232**, 780–788.

Narsinh, K.H., Sun, N., Sanchez-Freire, V., Lee, A.S., Almeida, P., Hu, S., Jan, T., Wilson, K.D., Leong, D., Rosenberg, J., Yao, M., Robbins, R.C. & Wu, J.C. (2011) Single cell transcriptional profiling reveals heterogeneity of human induced pluripotent stem cells. *J. Clin. Invest.* **121**, 1217–1221.

Overholtzer, M. & Brugge, J.S. (2008) The cell biology of cell-in-cell structures. *Nat. Rev. Mol. Cell Biol.* **9**, 796–809.

Overholtzer, M., Mailleux, A.A., Mouneimne, G., Normand, G., Schnitt, S.J., King, R.W., Cibas, E.S. & Brugge, J.S. (2007) A nonapoptotic cell death process, entosis, that occurs by cell-in-cell invasion. *Cell* **131**, 966–979.

R Core Team (2013) *R: A Language and Environment for Statistical Computing*. R Foundation for Statistical Computing, Vienna, Austria. http://www.R-project.org/

Ritter, M.A., Sauvage, C.A. & Cotmore, S.F. (1981) The human thymus microenvironment: in vivo identification of thymic nurse cells and other antigenically-distinct subpopulations of epithelial cells. *Immunology* **44**, 439–446.

Schmitt, A., Jouault, H., Guichard, J., Wendling, F., Drouin, A. & Cramer, E.M. (2000) Pathologic interaction between megakaryocytes and polymorphonuclear leukocytes in myelofibrosis. *Blood* **96**, 1342–1347.

Sharma, N. & Dey, P. (2011) Cell cannibalism and cancer. *Diagn. Cytopathol.* **39**, 229–233.

Steinhaus, J. (1981) Ueber carcinoma-einschlusse. *Virchows Arch.* **126**, 533–535.

Takeda, K. & Akira, S. (2001) Roles of Toll-like receptors in innate immune responses. *Genes Cells* **6**, 733–742.

Takeuchi, M., Inoue, T., Otani, T., Yamasaki, F., Nakamura, S. & Kibata, M. (2010) Cell-in-cell structures formed between human cancer cell lines and the cytotoxic regulatory T-cell line HOZOT. *J. Mol. Cell Biol.* **2**, 139–151.

Wekerle, H. & Ketelsen, U.P. (1980) Thymic nurse cells–Ia-bearing epithelium involved in T-lymphocyte differentiation? *Nature* **283**, 402–404.

Woulfe, D.S., Lilliendahl, J.K., August, S., Rauova, L., Kowalska, M.A., Abrink, M., Pejler, G., White, J.G. & Schick, B.P. (2008) Serglycin proteoglycan deletion induces defects in platelet aggregation and thrombus formation in mice. *Blood* **111**, 3458–3467.

Zientek-Targosz, H., Kunnev, D., Hawthorn, L., Venkov, M., Matsui, S., Cheney, R.T. & Ionov, Y. (2008) Transformation of MCF-10A cells by random mutagenesis with frameshift mutagen ICR191: a model for identifying candidate breast-tumor suppressors. *Mol. Cancer* **7**, 51.

Received: 30 January 2013
Accepted: 13 August 2013

Supporting Information

Additional Supporting Information may be found in the online version of this article at the publisher's web site:

Figure S1 Growth sensitivity of HCT116 to ICR-191. HCT116 cells were treated with ICR-191 (final 2, 5 or 10 μg/mL) for 8 h, and cultured with fresh medium for 1 day. Cell counting was performed using the Cell Counting Kit (Dojindo, Kumamoto, Japan), and the cells showed 50% survival around 6.2 μg/mL of ICR-191.

Movie S1 A representative cell-in-cell process in 9F-11A. This movie corresponds to the montage images shown in Fig. 2E. Bar = 20 μm.

Movie S2 Internalization process of multiple cells in 9F-11A. This movie corresponds to the montage images shown in Fig. 4A. Bar = 20 μm.

Movie S3 Pseudopodial dynamics during the process of appearance of cell-in-cell structures in 9F-11A. This movie corresponds to the montage images shown in Fig. 4B. Bar = 20 μm.

Movie S4 Pseudopodial dynamics during the process of appearance of cell-in-cell structures in 9F-11A. Bar = 20 μm.